Functional interactions between the cerebellum and the premotor cortex for error correction during the slow rate force production task: an fMRI study

Yoshiyuki Tanaka [a]*, Naoki Fujimura [a], Toshio Tsuji [a], Masaharu Maruishi [b], Hiroyuki Muranaka [b] and Tatsuya Kasai [c]

a Department of Artificial Complex Systems Engineering, Graduate School of Engineering, Hiroshima University, 1-4-1 Kagamiyama, Higashi-hiroshima 739-8527, Japan

b Division of Rehabilitation Medicine, Hiroshima Prefectural Rehabilitation Center, 295-3 Taguchi, Saijo, Higashi-hiroshima 739-0036, Japan

c Division of Sports and Health Sciences, Graduate School for International Development and Cooperation, Hiroshima University, 1-5-1 Kagamiyama, Higashi-hiroshima 739-8529, Japan

Email: ytanaka@bsys.hiroshima-u.ac.jp

Tel: +81-82-424-5763, Fax: +81-82-424-2387

Abstract

Although neuroimaging studies indicate that fMRI signal changes in the cerebellum (CB) during the performance of a target movement reflect functions of error detection and correction, it is not well known how the CB intervenes in task-demanded movement attributes during automated on-line movement, i.e., how the CB simultaneously coordinates movement rate and error correction. The present study was undertaken to address this issue by recording fMRI signals during the performance of a task at two different movement rates (0.4 Hz and 0.8 Hz). The results showed that movement errors increased with increasing movement rates. We also demonstrated that activation of the left CB increased with decreasing movement rates, whereas activation of the ipsilateral (right) premotor cortex (PMC) increased with increasing movement rates. Furthermore, there were significant relationships between individual movement errors and left CB activation at both movement rates, but these relationships were not observed in the ipsilateral PMC. Taken together, it is suggested that during the performance of automated and well-controlled slow force-production tasks, the interactions between cortical (right PMC) and subcortical (left CB) motor circuits, i.e., a functional dissociation between PMC and CB, is exclusively dedicated to controlling movement rate and error correction. In particular, the present results showing significant relationships between individual force-control errors and CB activation might reflect functional differences of an individual's internal model.

Keywords

Introduction

Many neuroimaging studies using positron emission tomography (PET) and functional magnetic resonance imaging (fMRI) have examined brain activation related to movement frequency (Van Meter et al. 1995; Sadato et al. 1996a; Jenkins et al. 1997; Jäncke et al. 1998; Riecker et al. 2003) and to movement velocity (Winstein et al. 1997; Turner et al. 1998, 2003; Desmurget et al. 2004). The results of regional cerebral blood flow (rCBF) studies obtained by tracking wrist movement showed that increasing activation in the supplementary motor area (SMA), the primary motor cortex (M1), the premotor cortex (PMC), the thalamus and the cerebellum (CB) was related to movement frequency (Van Meter et al. 1995). Turner et al. (2003) indicated that rCBF in the basal ganglia (BG), the CB, and the sensory motor cortex (SMC) are directly related to movement velocity and movement extent in the pursuit tracking task under different control-display gains . With regard to repetitive and sequential finger movement rates, Sadato et al. (1996a, b) demonstrated that there was a rapid rise in rCBF between the slow and the fast movement rates, but no further increase at the very fast rates. In addition, changes in the left SMC and CB likely reflect movement rate (Blinkenberg et al. 1996). Furthermore, a positive linear relationship between movement rate and fMRI signal change was also observed (Rao et al. 1993, 1996; Schlaug et al. 1996). Based on these findings, there is general agreement that both the SMA and the PMC appear to have an important role in the generation of sequences from memory that fit into a precise timing plan. However, no conclusive data exist on the interactions between movement rate and error correction.

In performing actual movements, predictive functions play an important role in automated on-line movement control, whereas there is general consensus that forward internal models are a fundamental principle in predictive motor control (Kawato 1999; Doya 1999, 2000). In addition, there is evidence that internal models are represented in the CB (Imamizu et al. 2000, 2003). Recently, Boecker et al. (2005) demonstrated the existence of modular representations for predictive force coupling, with the ipsilateral CB playing a major role. However, no conclusive data exist on automated procedures involving movement rate and error correction. In particular, it is not well understood how the CB handles a

behavioral situation when the specific internal models are induced by changes in movement rate and in movement error correction.

Hence, the present study was undertaken to address this issue and to investigate the central representation of internal models for automated force production by different movement rates. That is, how the CB contributes to automated error correction accompanied by different movement rates.

Methods

Subjects

Seven right-handed subjects (all Japanese males, 22 to 37 years of age), who surly used the right hand for wiring and manipulating a tool in their daily activities (Oldfield 1971) and did not suffer from any known neuromuscular disorders, participated in the present study after giving written informed consent in accordance with the Institutional Review Board. The ethical committee of the Hiroshima Prefectural Rehabilitation Center approved the experimental procedure for fMRI acquisition in this research study.

Experimental system

Figure 1a shows a schematic representation of the developed manual tracking system for evaluating error correction in the fMRI environment. This system was composed of an fMRI-compatible optical force sensor to measure the force exerted by right index finger abduction (Fig. 1b). The feedback display presented force errors, e, between the reference signal, fr, and the measured force signal, f, with the position of a white circle on the black screen window, and the circle moved up and down in real time (Fig. 1a). If the subject could completely follow the reference signal, the circle was always located at the desired point on the display. The system recorded the force produced by a subject with 1 kHz sampling frequency, and subjects did not notice a time delay in manipulating the force sensor to perform the force production task.

The force error correction task by using the right index finger was carried out for a sine-wave-like force change with amplitude 1.0 N on the base line of 2.0 N.

All subjects laid face up and used their right index fingers to touch the specified part of the optical force sensor, which was tightly fixed to a wooden plate (Fig. 1b). They were instructed to follow the reference signal by positioning the circle at the desired point (no error level) by using the visual feedback information.

In the fMRI experiments, all magnetic materials, such as the computer unit, were installed outside the scan room as shown in Fig. 1a (see also Maruishi et al. 2004). The optical fibers of the force sensor were connected to the computer unit through a waveguide in the scan room. The visual feedback information was projected onto the fMRI-compatible back-projection screen through the waveguide by a projector outside the scan room.

Experimental design

The influence of the frequency of a reference signal on motor performance and brain activation were examined by using the developed experimental system in the error correction task. In the present study, force production movement signal frequencies were 0.4 and 0.8 Hz. It is known that there is a rapid rise in rCBF between the slow and the fast movement rates, whereas no further increase of the very fast movement rates (Sadato et al. 1996a). In addition, there is a limitation in human ability to correcting errors under the conditions of tracking-like movement. Participants practiced for at least a five minutes to familiarize themselves with the two different frequencies.

In the fMRI experiment, the subject closed his eyes and displayed no motor activity for one minute in the "REST" condition, and then performed the error-correction task according to the visual feedback information projected on the screen for one minute in the "MOTION" condition. Each scan session lasted 5 min and proceeded along the following designed block paradigm: REST – MOTION – REST – MOTION – REST. The start and end commands for MOTION were delivered to the subject by using an fMRI-compatible headphone.

fMRI acquisition

The fMRI experiment was conducted on a 1.5-T SYMPHONY system with a head-coil (Siemens, Erlangen, Germany). We collected T2*-weighted transverse

echo–planar images (EPI) (FOV, 192 × 192 mm; matrix size, 64 × 64; in-plane resolution, 3 × 3 mm; flip angle, 90°; TE, 60 ms) with blood oxygenation level-dependent (BOLD) contrast. Twenty-four contiguous axial slices of 6-mm thickness were collected in each volume by using an interleaf method. An automatic shimming procedure was performed before each scan session. In each session, fifty-one functional volumes were collected within a single scanning session with an effective repetition time (TR) of 6.0 s/vol. The first volumes obtained in the sessions were discarded to allow for T1 equilibration effects (see Maruishi et al. 2004).

Behavioral data analysis

Motor performance in each session was quantitatively evaluated by using the total sum of force errors during two MOTION periods, E, defined as

$$E = \sum_{i=1}^{N} e(i)\Delta t$$

where Δt is the sampling time of the data measurement and N is the number of data measured in the MOTION periods.

fMRI data analysis

Preprocessing and statistical analyses of fMRI data were performed by using SPM2 software (Wellcome Department of Imaging Neuroscience, London, UK; http://fil.ion.ucl.ac.uk/spm/) implemented in MATLAB 7.0 (Mathworks, Sherborn, MA). Images were realigned to the first volume of the EPI time-series by using rigid-body transformation. Volumes were then normalized to the Montreal Neurological Institute (MNI) template by using linear affine transformations. Normalized images of 3 × 3 × 6 mm were spatially smoothed by a Gaussian kernel of 8-mm full-width at half-maximum (FWHM). Areas of significant change in the brain were estimated by using the general liner model (GLM) in a blocked design of the contexts, convolved with the hemodynamic response function (HRF). Temporal filtering was achieved by using autoregressive modeling (AR(1)) to model high-frequency noise, and a high-pass filter (cutoff: 128 Hz) was applied to remove low-frequency noise.

Direct comparisons between the contexts were conducted to find brain activations that were greater at the higher frequency than at the lower frequency (0.8 Hz versus 0.4 Hz) as well as those that were greater at the lower frequency than at the higher frequency (0.4 Hz versus 0.8 Hz). We analyzed the time series of the images obtained from the seven subjects as one group to increase the sensitivity of the fMRI analysis. This implies that the statistical analyses used in the present study are group fixed-effect analyses ($p < 0.001$, uncorrected). Anatomical identification was carried out by superimposing the maximum activation foci both on the MNI template and on the normalized structural images of each subject. Anatomical labels of activated regions were made based on the atlas of Talairach and Tournoux (1988) by Talairach Daemon (http://www.talairach.org/index.html), after a nonlinear coordinate transformation from MNI to Talairach coordinates (Brett et al. 2001). The location of the dentate nucleus was reconfirmed by using an MRI atlas of the cerebellar nuclei (Dimitrova et al., 2006).

In addition, based on results of the whole-brain analysis, local region-of-interest (ROI) analysis was carried out by using the Marsbar toolbox (Brett et al. 2002; http://marsbar.sourceforge.net) to further investigate brain activations within each noted region. Each ROI was defined as the location of the peak voxel in each region, and was generated by taking a spherical mask surrounding the peak voxel with an 8 mm diameter. We then calculated the percent signal change (PSC) from the time course of hemodynamic response (HDR) in each subject. Subject C's PSC in the CB for 0.8 Hz was discarded in calculating correlation because his outlier was beyond the level of two-SD.

Results

Motor performance

Table 1 shows individual values of the force errors, *E*, calculated from the recorded data for the two reference frequencies, 0.8 Hz and 0.4 Hz. The effect due to frequencies was statistically significant, as the effect was larger at 0.8 Hz ($p <$

0.05). From self-reports obtained from each subject, all subjects felt that it was easier to correct errors at 0.4 Hz than it was at 0.8 Hz.

fMRI

Table 2 summaries the results of fMRI analyses on anatomical location, MINI coordinates, the activated voxel counts and the peak intensity (maximum Z-score), demonstrating clusters that were significant for direct contrasts in a couple of conditions (uncorrected, $p < 0.001$). A comparison of the 0.8 Hz results with the 0.4 Hz results revealed that the magnitude of activation in the bilateral PMC significantly increased in proportion to the frequency of a reference signal, whereas foci of activity also could be found in the right M1, the insula, Broca's area, and CB (see also Fig. 2a). This result follows the previous studies on rate-effect that activations of PMC and CB increase in proportional to movement rate during voluntary movements (cf. Van Meter et al. 1995). On the other hand, the left CB, including the dentate nucleus and tonsil, were more strongly activated at the lower signal frequency than for the higher signal frequency (Fig. 2b). Activations of these cerebellar regions during simple finger movement tasks were reported in previous studies (cf. Penhune and Doyon 2005).

Two ROIs were selected based on Table 2, where both the number of voxels and the Z-value were largest in each of the direct comparisons. The first ROI was the region including the right PMC ($x = 58$, $y = 0$, $z = 46$) and the second was found in the left CB ($x = –18$, $y = –52$, $z = –38$). Figs. 2c and 2d show the relationships between local activations in the two regions and motor performance during movement tasks, respectively. The local activations in the right PMC for 0.8 Hz tended to be larger than for 0.4 Hz, but there was no significant relationship between individual local activations and the amount of movement errors (Fig. 2c). In the left CB, on the other hand, there were significant positive-linear relationships between them for both reference frequencies, whereas the regression coefficient in the case of 0.4 Hz was larger than in the case of 0.8 Hz (Fig. 2d). These results indicated that the CB might play an important role in error correction and that the individual differences of this function reflect brain activation.

Discussion

Action monitoring and error detection are processes that are necessary to adapt motor behavior to the requirements of the current task to be performed. In the present study, therefore, to investigate the relationship between brain activation and movement error correction, we used a force-error correction system that simultaneously and correctly recorded fMRI signals and force errors. Although both functions of the PMC and the CB are triggered by the external signal and it is well known that functions of the CB were deeply related to movement speed, the present results show that the movement-related M1 activity is similar to muscle activity. That is, the present study is consistent with previous findings, confirming that M1 activity is closely related to movement. In addition, the present results show that force errors correspondingly increased with increasing movement rates. Activation of the left CB increased depending on a decrease in the movement rate, whereas activation of the ipsilateral (right) PMC increased depending on increasing movement rates. Furthermore, there were statistically significant relationships between individual force errors and CB activations in both movement rates, but these relationships were not observed in the ipsilateral (right) PMC. Based on these results, human neural mechanisms are related to intervention between error corrections and movement rates.

As described above, the results of the fMRI study demonstrate that ipsilateral PMC and left CB activities definitely changed during error correction movements. In particular, ipsilateral PMC activations increased with an increasing movement rate. Surprisingly, however, CB activations did not increase with increasing movement rates, but instead increased with a lower movement rate. Thus, activation changes in the PMC and the CB with different movement rates might be interpreted as functional interactions because it is known that both activities are related to voluntary movements induced by an external trigger (cf. Porter and Lemon 1993). Although the ipsilateral PMC is sensitive to changes of the movement rate, the CB plays a dominant role in error correction in slow and well-controlled movement. It is expected that these tendencies observed in the right finger will be sharpened when the subjects perform with the left index finger, because subdominant hand movements cause an increase of activity in the CB (Jäncke et al., 1999; Taniwaki et al., 2006). Recently, by using PET, Penhune and Doyon (2005) demonstrated that activity in the CB hemispheres early in learning

is likely related to error correction mechanisms that optimize movement kinematics, resulting in improved performance. The present results related to activation in the CB hemispheres, especially the left CB, could be explained in line with the above-mentioned similar activity. The present sequential movement was simple and similar to situations experienced early in learning, especially for the case of the slower movement rate (0.4 Hz). This evidence indicates that there are functional interactions between these two motor cortices that might correspond to different movement rates. In other words, this functional interaction is modulated by task-demanded movement attributes, such as the speed/accuracy trade-off phenomenon (Plamondon and Alimi 1997). In fact, the subjects felt that it was more difficult to correct force errors at the higher frequency because they had to concentrate on gauging the rapid change of errors via the visual feedback display rather than concentrating on controlling their finger motion. They did not know if their motor outputs were helping to reduce errors. On the other hand, all of them felt that it was easy to gauge and correct errors at the lower frequency because they had time to precisely control their motion in response to the error information. These results indicate that the CB works more effectively for learning when the change of error information is harmonized with voluntary motor output as well as sensory input, whereas the PMC activates to compensate the subjective gap between expectations and results. It is suggested that the PMC and the CB play an important role in this movement law and the present results of both brain activations might reflect functional interactions.

The novel finding of the present study was that the amount of individual errors at both movement rates were significantly related to individual CB activations. The CB has traditionally been viewed as an integral part of the motor system (Raymond et al. 1996). CB activation is highly correlated with the SMC since they are involved in the somatosensory feedback of the movement, organizing a perfect transfer of the internal image of the movement into the actual physical conditions of the external world. Therefore, new perspectives on CB function are closely linked to the emergence of cognitive function (attention shifting, Allen et al. 1997; memory rehearsal, Desmond et al. 1997; sensory exploration, Gao et al. 1996). In the present study, there were significant relationships between individual force errors and CB activations. One possible explanation for the present results, therefore, could be in line with viewpoints of internal model

hypotheses related to cognitive neuroscience. That is, the CB neurons related to individual abilities in error correction correspond to individual visual affective input and rapidly prime task-relevant systems in order to enhance neural responsiveness (Allen et al. 1997). In the present study, subjects with large force errors showed higher CB activation and vice versa. This evidence indicates that the subjects with a more highly functional internal model produce few errors and do not need higher CB activation. That is, these subjects could automatically perform the task. This mental effort did not activate the CB. Thus, the significant relationships between individual force errors and CB activation might reflect functional differences in individual internal models developed by different subjects.

On the other hand, it is suggested that the PMC may have a role in preprogrammed processes linked to sequential motor actions, and therefore have an important role in the generation of sequences from memory that fit into a precise timing plan. In particular, the right PMC (ipsilateral PMC in the present study) has a role in working memory (Sadato et al. 1996b). As described above in the low movement rate study, there were no relationships between individual force errors and ipsilateral PMC activation. This evidence suggests that interactions of the PMC and the CB are induced by performing the error correction task, but offer a potentially causal link between them for on-line performance of error correction at different movement rates. In particular, the present evidence suggests the idea that when an error is detected at the slower movement rate, descending output from the CB nuclei allows for rapid, on-line adjustments in the motor patterns without requiring extensive cortical intervention. This error correction hypothesis implicitly assumes that the CB has evolved so that it can now provide a more genetic error correction role, modified by an individual's internal model in addition to external movement (Ivry and Fiez 2000).

With regard to the neural mechanisms of the interactions between the cortical (PMC) and the subcortical (CB) motor circuits, the present results suggest that these motor circuits are exclusively devoted to controlling movement rate and error correction. More recently, using fMRI, Galléa et al. (2008) demonstrated that supplementary motor area (SMA) and dorsal anterior cingulate cortex (ACC) activation increased with error and task difficulty independent of the accuracy of

motor control. Similarly, the present results suggest a clear functional dissociation between PMC and CB in controlling movement rate and error correction and have provided new insights into the interactions between actions and cognition. Thus, our findings in the present study have confirmed above-mentioned broad functional implications, but more investigations are needed to clarify further neural mechanisms related to human error correction and the control of movement rate. The use of an online motor control paradigm eliciting errors allowed us to show error-related brain activity pattern independent to decision making.

Reference

Allen G, Buxton RB, Wong EC, Courchesne E (1997) Attention activation of the cerebellum independent of motor involvement. Science 275: 1940-1943

Blinkenberg M, Bonde C, Holm S, Svarer C, Andersen J, Paulson OB, Law I (1996) Rate dependence of regional cerebral activation during performance of a repetitive motor task: A PET study. J Cerb Blood Flow Metab 16: 794-803

Boecker H, Lee A, Muhlau M, Ceballos-Baumann A, Ritzl A, Spilker ME, Marquart C, Hermsdorfer J (2005) Force level independent representations of predictive grip force-load force coupling: a PET activation study. NeuroImage 25: 243-252

Brett M, Christiff K, Cusack R, Lancaster J (2001) Using the Talairach atlas with the MNI template. NeuroImage 13: S85

Brett M, Anton J, Valabregue R, Poline J (2002) Region of interest analysis using an SPM toolbox [abstract]. Presented at HBM2002 16, 2002. Available on CD-ROM in NeuroImage

Deiber M, Honda M, Ibañez V, Sadato N, Hallett M (1999) Mesial motor areas in self-initiated versus externally triggered movements examined with fMRI: Effect of movement type and rate. J Neurophysiol 81: 3065-3077

Desmond JE, Gabrieli DE, Wagner AD, Ginier BL, Glover GH (1997) Lobular patterns of cerebellar activation in verbal working-memory and finger-tapping tasks as revealed by functional MRI. J Neurosci 17: 9675-9685

Desmurget M, Grafton ST, Vindras P, Grea H, Turner RS (2004) The basal ganglia network mediates the planning of movement amplitude. Europ J Neurosci 19: 2871-2880

Dimitrova A, Zeljko D, Schwarze F, Maschke M, Gerwig M, Frings M, Beck A, Aurich V, Forsting M. Timmann D (2006) Probabilistic 3D MRI atlas of the human cerebellar dentate/interposed nuclei. NeuroImage 30: 12-25

Doya K (1999) What are the computations of the cerebellum, the basal ganglia, and the cerebral cortex? Neural Networks 12: 961-974

Doya K (2000) Complementary roles of basal ganglia and cerebellum in learning and motor control. Curr Opin Neurobiol 10: 732-739

Galléa C, Graaf JB, Pailhous J, Bonnard M (2008) Error processing during online motor control depends on the response accuracy. Behav Brain Res 193: 117-125

Gao JH, Parson LM, Bower JM, Xiong J, Li J, Fox PT (1996) Cerebellar implicated in sensory acquisition and discrimination rather than motor control. Science 272: 545-547

Imamizu H, Miyauchi S, Tamada T, Sasaki Y, Takino R, Putz B, Yoshioka T, Kawato M (2000) Human cerebellar activity reflecting an acquired internal model of a new tool. Nature 403: 192-195

Imamizu H, Kuroda T, Miyauchi S, Yoshida T, Kawato M (2003) Modular organization of internal models of tools in the human cerebellum. Proc. Natl Acad Sci U.S.A. 100: 5461-5466

Ivry RB, Fiez JA (2000) Cerebellar contributions to cognition and imagery. In: Gazzaniga MS (ed) The new cognitive neurosciences. MIT Press, pp 999-1011

Jäncke L, Specht K, Mirzazade S, Loose R, Himmelbach M, Lutz K, Shah NJ (1998) A parametric analysis of the 'rate effect' in the sensorimotor cortex: a functional magnetic resonance imaging analysis in human subjects. Neurosci Lett 252: 37-40

Jäncke L, Specht K, Mirzazade S, Peters M (1999) The effect of finger-movement speed of the dominant and the subdominant hand on cerebellar activation: a functional magnetic resonance imaging study. NeuroImage 9: 497-507

Jenkins IH, Passingham RE, Brooks DJ (1997) The effect of movement frequency on cerebral activation: a positron emission tomography study. J Neurol Sci 151: 195-205

Kawato M (1999) Internal models for motor control and trajectory planning. Curr Opin Neurobiol 9: 718-727

Maruishi M, Tanaka Y, Muranaka H, Tsuji T, Ozawa Y, Imaizumi S, Miyatani M, Kawahara J (2004) Brain activation during manipulation of the myoelectric prosthetic hand: a functional magnetic resonance imaging study. NeuroImage 21: 1604-1611

Oldfield RC (1971) The assessment and analysis of handedness: the Edinburgh inventory. Neuropsychologia 9: 97-113

Penhune VB, Doyon J. (2005) Cerebellum and M1 interaction during early learning of timed motor sequences. NeuroImage 26: 801-812

Plamondon R, Halimi AM (1997) Speed/accuracy trade-offs in target-directed movements. Behav Brain Sci 20: 279-349

Porter R, Lemon R (1993) Corticospinal function and voluntary movement. Clarendon Press, Oxford.

Rao SM, Binder JR, Bandettini PA, Hammeke TA, Yetkin FZ, Jesmanowicz A, Lisk LM, Morris GL, Mueller WM, Estkowski LD, Wong EC, Haughton VM, Hyde JS (1993) Functional magnetic resonance imaging of complex human movements. Neurol 43: 2311-2318

Rao SM, Bandettini PA, Binder JR, Bobholz JA, Hammeke TA, Stein EA, Hyde JS (1996) Relationship between finger movement rate and functional magnetic resonance signal change in human primary motor cortex. J Cereb Blood Flow Metab 16: 1250-1254

Raymond JL, Lisberger SG, Mauk MD (1996) The cerebellum: a neural learning machine? Science 272: 1126-1131

Riecker A, Wildgruber D, Mathiak K, Grodd W, Ackermann H (2003) Parametric analysis of rate-dependent hemodynamic response functions of cortical and subcortical brain structures during auditorily cued finger tapping: a fMRI study. NeuroImage 18: 731-739

Sadato N, Ibanez V, Campbell G, Leonardo M, Hallett M (1996a) Frequency-dependent changes of regional cerebral blood flow during finger movements. J Cereb Blood Flow Metab 16: 23-33

Sadato N, Campbell G, Ibanez V, Deiber M, Hallett M (1996b) Complexity affects regional cerebral blood flow change during sequential finger movements. J Neurosci 16: 2691-2700

Schlaug G, Sanes JN, Thangaraj V, Darby DG, Jäncke L, Edelman RR, Warach S (1996) Cerebral activation covaries with movement rate. NeuroRep 7: 879-883

Talairach J, Tournoux P (1988) Co-planar stereotaxic atlas of the human brain. Thieme, New York

Taniwaki T, Okayama A, Yoshiura T, Togao O, Nakamura Y, Yamasaki T, Ogata K, Shigeto H, Ohyagi Y, Kira J, Tobimatsu S (2006) Functional network of the basel ganglia and cerebellar motor loops in vivo: different activation patterns between self-initiated and externally triggered movements. NeuroImage 31: 745-753

Turner RS, Grafton ST, Votaw JR, Delong MR, Hoffman JM (1998) Motor subcircuits mediating the control of movement velocity: a PET study. J Neurophysiol 80: 2162-2176

Turner RS, Desmurget M, Grethe J, Crutcher MD, Grafton ST (2003) Motor subcircuits mediating the control of movement extent and speed. J. Neurophysiol 90: 3958-3966

VanMeter JW, Maisog JM, Zeffiro TA, Hallett M, Herscovitch P, Rapoport SI (1995) Parametric analysis of functional neuroimages: application to a variable-rate motor task. Neuroimage 2: 273-283

Winstein CJ, Grafton ST, Pohl PS (1997) Motor task difficulty and brain activity: investigation of goal-directed reciprocal aiming using positron emission tomography. J Neurophysiol 77: 1581-1594

Figure legends

Fig 1. Experimental setup.   **a** Experimental apparatus under an fMRI environment.   **b** Optical force sensor for measuring the force applied by an index finger.

Fig 2. Results from direct comparisons between task conditions of a reference signal frequency (p < 0.001, uncorrected) and region of interest (ROI) analysis. The arrow indicates the center of ROI. **a** Greater activations in the direct comparison of 0.8 Hz with 0.4 Hz.   **b** Greater activations in the direct comparison of 0.4 Hz with 0.8 Hz.   **c** Relationships between local brain activations and individual force errors in the right PMC at two different movement frequencies (0.4 Hz and 0.8 Hz). A vertical length is PSCs and a horizontal side is force errors.   **d** Relationships between them in the left CB. All representations are same as Fig. 2c. However, Subject C's PSC in the CB for 0.8 Hz (the black square with sharp-mark) was discarded in calculating correlation because his outlier was beyond the level of two-SD.

Tables

Table 1. Force errors in the two different rates of a reference signal.

Subject		A	B	C	D	E	F	G	Mean ± SD
Force errors, E [Ns]	0.4 Hz	40.83	48.81	26.51	43.49	30.81	37.83	55.10	40.48 ± 9.9
	0.8 Hz	89.53	47.61	34.47	53.73	45.29	40.51	64.41	53.65 ± 18.48
Absolute difference		48.7	1.19	7.96	10.24	14.48	2.68	9.31	13.17 ± 15.27*

Note: Data obtained from the first six seconds in each MOTION period was discarded because of the delay of subject's response to the starting signal. $*p < 0.05$.

Table 2. Anatomical localizations, activated voxels, and *Z* scores of the peak activation that showed a significant difference in direct comparisons between task conditions.

Lobe	Anatomical region	BA	x	y	z	Voxels	Z-Value
0.8Hz-0.4Hz							
Frontal	R. Middle frontal gyrus	6	58	0	46	435	4.82
	R. Superior frontal gyrus	6	20	-18	74	29	4.05
	R. Superior frontal gyrus	-	18	-2	76	13	3.62
	R. Precentral gyrus	6/4	46	-10	64	155	4.03
	L. Precentral gyrus	6	-62	6	22	20	3.89
	L. Precentral gyrus	6	-44	-10	36	32	3.63
	R. Middle frontal gyrus	6	8	-4	62	16	3.48
	L. Middle frontal gyrus	6	-32	12	64	11	3.55
	L. Middle frontal gyrus	6	-24	18	64	12	3.4
Parietal	R. Postcentral gyrus	43	68	-12	20	38	4.13
Limbic	R. Parahippocampal gyrus	-	26	-6	-16	38	3.87
Sub-lobar	R. Insula	13	40	-16	14	17	3.45
	R. Extra-nuclear	13	44	8	-10	12	3.33
Anterior	R. Cerebellum	-	18	-32	-24	15	3.59
0.4Hz-0.8Hz							
Anterior	L. Cerebellum	-	-18	-52	-38	127	5.19
Frontal	R. Inferior frontal gyrus	47	32	34	-20	12	4.03

Note: x, y, z coordinates relate to MNI stereotaxic space (negative and positive x values indicate the left and right hemispheres respectively). Brodmann areas are prefixed with BA. All activations were at $p < 0.001$ (uncorrected, 10 voxel cluster size).
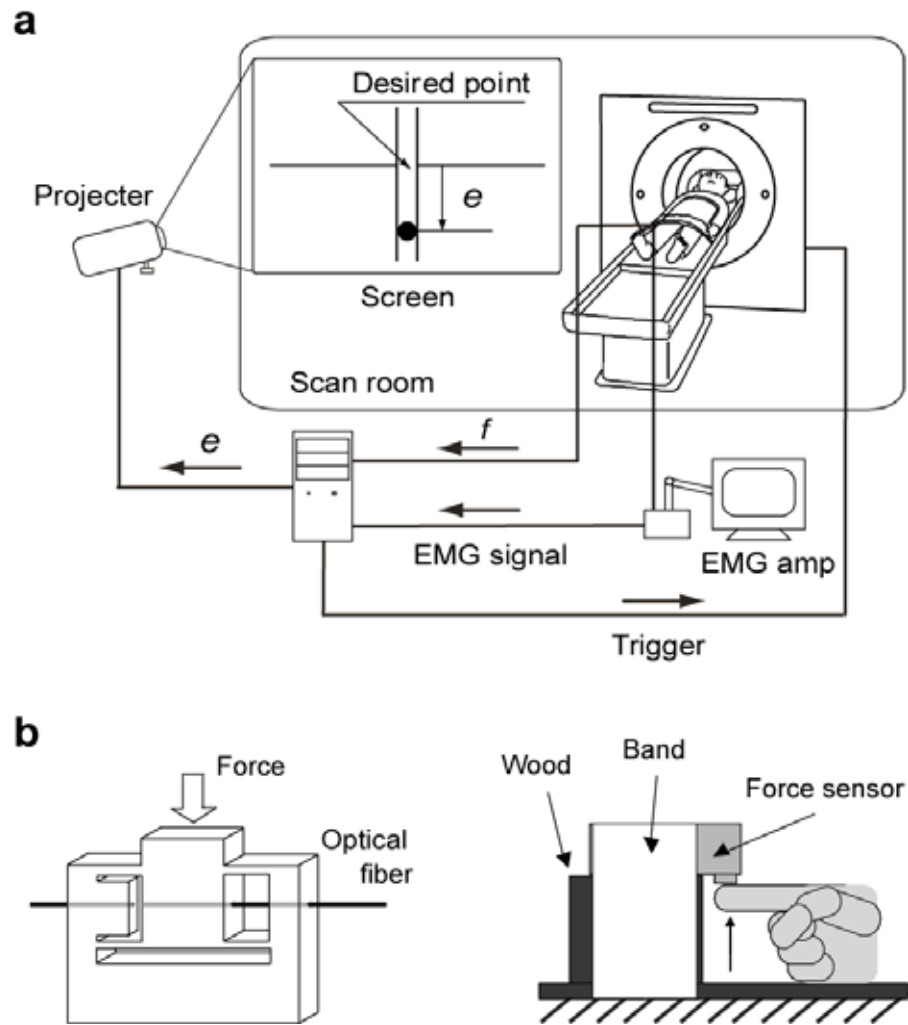
Figures

Fig. 1

Fig. 2

a

0.8Hz
- 0.4Hz

P   A   L   R   P   A

L

R

b

0.4Hz
- 0.8Hz

Sagittal   Coronal   Transverse

c

d

y = 0.0285x - 0.858

y = 0.004x - 0.340

19